Analytical MTF Bounds and Estimate for SFR in Discrete Imaging Arrays Due to Non-Stationary Effects

R. Jenkin,* R. E. Jacobson,▲ M. A. Richardson,* and I. C. Luckraft***

**Electro-Optics Group, Cranfield University, The Defence Academy, Shrivenham, Swindon, United Kingdom*

***Imaging Technology Research Group, University of Westminster, Watford Road, Harrow, Middlesex, United Kingdom*

Formulae are derived which calculate the bounds of discrete array MTF caused by the non-stationary nature of such devices. It is shown that if the traditional sinc based description of discrete device MTF is used, overestimation occurs. The average of the derived bounds is shown to be a good estimate of the SFR of the device. The formulae are tested against the performance yielded by a commercially available electronic still camera using a Sine wave, Edge and ISO Standard 12233 methods. Confidence limits calculated using the method detailed by Yeadon, Jones and Kelly and sources of errors are discussed. It is suggested that the presented formulae provide a better indication of discrete array performance for inclusion in system design for critical applications.

Journal of Imaging Science and Technology 47: 200–208 (2003)

Introduction

A considerable contribution to the MTF of a discrete image acquisition device is made by the geometrical properties of the sampling matrix.[1] This is defined by the dimensions of the sampling elements and the frequency at which these elements occur.[2]

The introduction of geometrical sampling will cause a change in the MTF of the system with respect to these parameters. In addition, due to the use of rectangular pixels and sampling grids, the imaging system is rendered non-isotropic and non-stationary.[2] The PSF of the system will therefore change with respect to orientation and position within the field of view.[2]

There is a large variation in approach to the issue of the non-stationary and non-isotropic nature of discrete systems. Few models have been produced which consider these effects and those that exist are often difficult to implement. The most common expression used as the one-dimensional geometrical MTF of a discrete *array* is of the form [Ref. 3, page 208]:

$$MTF(\omega) = \frac{\sin(\pi s \omega)}{\pi s \omega} \tag{1}$$

where ω represents spatial frequency and s the size of the pixel aperture. The formula is misused as the MTF of an array because it only accounts for the frequency response of a single pixel. No allowance for the sampling pitch or phase differences between the test signal and sampling comb is made. This one dimensional representation does not therefore account for the non-stationary nature of these systems. Using this formula no difference in MTF would be predicted for frame and interline transfer devices with the same light sensitive pixel dimensions. The representation is often expanded to two dimensions:

$$MTF(u,v) = \frac{\sin(\pi u s)}{\pi u s} \cdot \frac{\sin(\pi v l)}{\pi v l} \tag{2}$$

where u and v represent spatial frequency in orthogonal directions (Ref. 3, page 240). As previously, the formula merely represents the frequency response of a single pixel. This work shows that without considering the effects of the sampling comb and phase, the MTF of a discrete device is overestimated. In turn this could have consequences for critical applications such as recording of fingerprints or identification of targets. There also exists a large body of work in a varied range of applications that could be affected by the effects of the non-stationary nature of discrete systems, see Refs. 4 through 7 for example. Susceptibility to error will vary across fields and would need to be determined.

The majority of variation in MTF for discrete devices is caused by phase differences between the signal and sampling comb. This has been considered and incorporated into treatments by Feltz and Karim[8] and also Balram.[9] Feltz and Karim consider the output from two neighboring pixels and define variables, ψ_H and ψ_L, which represent the offset between signal extrema and the nearest pixel center.[8] ψ_H corresponds to offset for maxima and ψ_L that for minima. Normalized pixel width, α, and array pitch, β, are calculated in the following manner:

Original manuscript received August 5, 2002

▲ IS&T Member

$$\alpha = \frac{\pi T_\alpha}{T_N} \tag{3}$$

$$\beta = \frac{\pi T_\beta}{T_N} \tag{4}$$

where T_α is pixel width, T_β array pitch and T_N the half period of the input signal (named Nyquist period by Feltz and Karim [8]).

Derivation proceeds by rewriting ψ_L in terms of ψ_H. A variable, ψ_H^*, is defined that represents a critical value of ψ_H at which signal minima lie at the boundary between the two pixels being considered. This is calculated by defining the pixel index under consideration:

$$n = Int\left[\frac{T_N}{\beta}\right] + 1 \tag{5}$$

where *Int* represents an integer truncation function. The critical offset is then determined as [8]:

$$\psi_H^* = \pi - \left(n - \frac{1}{2}\right)\beta \tag{6}$$

Feltz and Karim state that the above definitions allow ψ_L to be rewritten as:

$$\psi_L = \psi_H + k\beta \tag{7}$$

where

$$k = \begin{cases} n: & \Psi_H \le \Psi_H^* \\ n-1: & \Psi_H > \Psi_H^* \end{cases} \tag{8}$$

Recorded maxima and minima, B_{MAX} and B_{MIN}, for a sinusoidal exposure are then expressed as:

$$B_{\max} = \int_{\theta=\Psi_H-\frac{\alpha}{2}}^{\Psi_H+\frac{\alpha}{2}} 0.5[1+\cos(\theta)]d\theta \tag{9}$$

$$B_{\min} = \int_{\theta=\Psi_L-\frac{\alpha}{2}}^{\Psi_L+\frac{\alpha}{2}} 0.5[1+\cos(\theta)]d\theta \tag{10}$$

where θ is angular distance. The MTF of a discrete device, capturing static images, is then deduced to be[8]:

$$MTF = \frac{\sin\left(\frac{\alpha}{2}\right)\left[\cos(\psi_H) - \cos(\psi_H + k\beta)\right]}{\alpha + \sin\left(\frac{\alpha}{2}\right)\left[\cos(\psi_H) + \cos(\psi_H + k\beta)\right]} \tag{11}$$

Feltz and Karim continue the derivation to produce expressions for dynamic MTF,[8] i.e.,when the scene to be captured is moving with respect to a particular exposure time. This analytical approach was among the first published which incorporated the effects of array alignment into expressions for discrete device MTF. The use of a logical operator, an *if* statement, in the calcu-lation of k and the subsequent reliance on pixel indices to determine ψ_H and ψ_L, however, limits the use of this approach.

Mathematical manipulation and finding analytical equivalents for logical operators is difficult. This therefore constrains the reduction and simplification of expressions that incorporate them as well as the mathematical techniques that may be applied to the formulae. Further, calculation of functions that incorporate these operators is often cumbersome.

Using the above approach it is difficult to calculate extremes of array performance. This is because, as ψ_H is specified, the formulae only indicate the pixel index that should be under consideration and no other information. Graphs of MTF versus ψ_H need to be produced to determine maximum and minimum response at each spatial frequency as in Ref. 8.

In addition, the above calculation will only be valid for the locale of the two pixels that Feltz and Karim consider. It may reasonably be expected that any nontrivial physical device will encounter the full range of possible values for ψ_H and ψ_L within its field of view. The only exception to this is if the spatial frequency of the signal is an integer multiple of the array pitch and aligned precisely with one axis of the sampling grid.

On the basis of the above, an argument may be formed that it is the range of performance of a particular device that is of more interest than the precise phase-MTF relationship. Certainly, for critical applications it is the minimum response that is of more interest.

At present the majority of sophisticated imaging applications, cannot yet account for local variations in MTF on a pixel by pixel basis. Therefore, reduction of device MTF to the maximum and minimum case provides an opportunity to calculate either maximum and minimum responses or to further deduce an average response and thus a mean output. This work details simple analytical expressions for discrete devices that describe extremes of array performance without inclusion of logical operators.

Mathematical Development

Assumptions and Exposure

To develop formulae that account for geometrical properties of a sampling array, it is assumed that the sampling process is noiseless as is the exposing signal. To further simplify derivation, this work is developed for the one-dimensional case. Development of the model commences with specification of a sinusoidal exposure distribution, $E(x)$, thus:

$$E(x) + a + b\cos(2\pi wx) \tag{12}$$

where ω is spatial frequency, x is distance, a the DC level and b the amplitude of the signal. The above distribution is allowed, metaphorically, to *fall* onto a sampling array that has sampling pitch p, sampling aperture s and behave according to the above constraints, Fig. 1. For the purposes of derivation it is also assumed that the array and signal extend infinitely.

Sampling

An idealized sampling element centered at spatial position u will collect incident light between u – s/2 and u + s/2, Fig. 1. Due to the initial assumptions, modeling the sampling of a single element may be represented

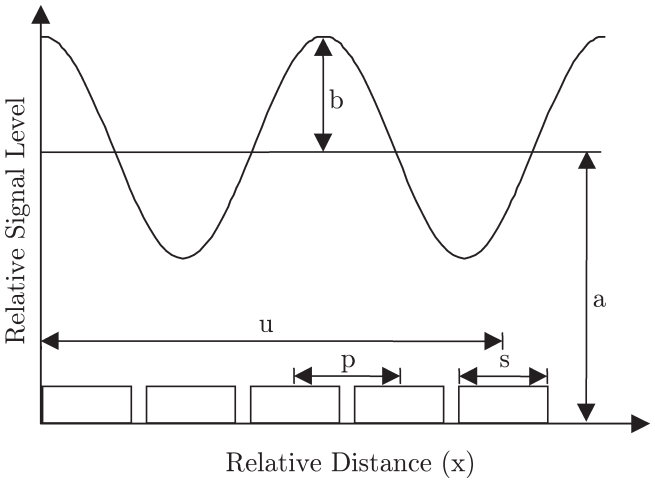

Figure 1. Signal and sampling array parameters.

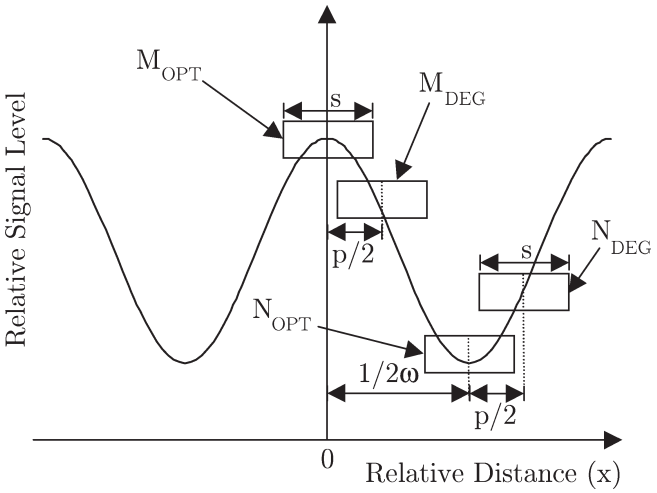

Figure 2. Coincidence of maxima and minima with sampling elements. Pitch and aperture are denoted s and p. M_{OPT} and N_{OPT} represent the optimum detection of maxima and minima. M_{DEG} and N_{DEG} represent the most degraded detection possible. Spatial frequency is ω.

by straightforward integration of the signal between these points. Thus, the response, $R(u,s)$ of a single element when sampling the above signal may be written:

$$R(u,s) = \int_{u-\frac{s}{2}}^{u+\frac{s}{2}} E(x)dx \tag{13}$$

The modulation of the signal recorded by the array is dependent upon the values recorded for the maxima and minima of the input signal.[8] Consequently this will be dependent upon the response of the element that is nearest the particular maximum or minimum in question and will vary according to its proximity.[8] Establishing the variation in the values of maxima and minima recorded will yield the geometrical MTF of the array and its effects due to phase differences between the sampling comb and signal.

Recording of Maxima and Minima

For an idealized pixel as above, the optimum recording of a maximum will occur when the center of a sampling element coincides with that maximum, Fig. 2. For the signal defined it may be shown that maxima occur at $x = n/\omega$, where n is an arbitrary positive integer. Therefore, a maximum is always present at $x = 0/\omega \equiv 0$. Thus, the optimum value of a maximum, M_{OPT}, that may be recorded for the defined signal when sampled by an element as defined above will be:

$$M_{OPT} = R(0,s)\int_{0-\frac{s}{2}}^{0+\frac{s}{2}} E(x)dx \tag{14}$$

The most degraded recording of a maximum will be dependent upon the pitch, p, of the sampling comb that will influence the proximity of the nearest element.

It may be shown that for a given sampling array, a pixel center will *always* fall within $p/2$ of a given maximum for signals below the Nyquist frequency of the device. A straightforward conclusion is that the furthest a pixel will be from a given maxima is $p/2$. The most degraded value recorded, M_{DEG}, for a given maximum sampled using an array of pitch, p will therefore be:

$$M_{DEG} = R(\frac{p}{2},s) = \int_{\frac{p}{2}-\frac{s}{2}}^{\frac{p}{2}+\frac{s}{2}} E(x)dx \tag{15}$$

Similarly, the recording of signal minima will also depend upon the pitch of the sampling array and the aperture of the sampling elements. Again, optimum recording will occur when the element center coincides with a minimum. It may be shown that as minima occur at $x = 1/2\omega + n/\omega$, a minima will exist at $x = 1/2\omega$. Therefore, the optimum value, N_{OPT}, recorded for a signal minimum will be:

$$N_{OPT} = R(\frac{1}{2\omega},s) = \int_{\frac{1}{2\omega}-\frac{s}{2}}^{\frac{1}{2\omega}+\frac{s}{2}} E(x)dx \tag{16}$$

As previously, it may be shown that the furthest an element center may exist from the minima is $p/2$ and therefore the most degraded recording of the minima, N_{DEG}, will be given by:

$$N_{DEG} = R\left(\frac{p}{2}+\frac{1}{2\omega},s\right) = \int_{\frac{p}{2}+\frac{1}{2\omega}-\frac{s}{2}}^{\frac{p}{2}+\frac{1}{2\omega}+\frac{s}{2}} E(x)dx \tag{17}$$

Signal Modulation

The modulation, MTF, of the recorded signal may now be calculated using[10]:

$$MTF = \frac{M-N}{M+N} \tag{18}$$

where M and N represent the recorded values for maxima and minima respectively for a given signal. The values derived above for recorded maxima and minima are used as extrema within the equation and a solution

derived to calculate the maximum and minimum of Eq. (18). For a non-trivial system and signal it may be assumed all recorded values are positive and that:

$$M_{OPT} > M_{DEG} > N_{DEG} > N_{OPT} \tag{19}$$

Employing the above and the elementary use of inequalities, it may be shown that the maximum and minimum recorded modulation of the signal, MTF_{MAX} and MTF_{MIN}, will be given by:

$$MTF_{MAX} = \frac{M_{OPT} - N_{OPT}}{M_{OPT} + N_{OPT}} \tag{20}$$

$$MTF_{MIN} = \frac{M_{DEG} - N_{DEG}}{M_{DEG} + N_{DEG}} \tag{21}$$

Expanding, then simplifying the above equations yields:

$$MTF_{MAX} = \frac{b\sin(\pi\omega s)}{a\pi\omega s} \tag{22}$$

$$MTF_{MIN} = \frac{b\cos(\pi\omega p)\sin(\pi\omega s)}{a\pi\omega s} \tag{23}$$

The average MTF of the sampling array may be calculated using the mean of Eqs. (22) and (23).

$$MTF_{AVE} = \frac{MTF_{MAX} + MTF_{MIN}}{2} \tag{24}$$

This may be expanded to:

$$MTF_{AVE} = \frac{b\cos^2\left(\frac{\pi\omega p}{2}\right)\sin(\pi\omega s)}{a\pi\omega s} \tag{25}$$

It should be noted that Eqs. (22), (23) and (25) yield absolute recorded modulation. It is normal practice to normalize the response with respect to the zero frequency (DC) component of the curve in order to produce the MTF. This may be achieved by omitting variables a and b in the above equations. The original assumption, Eq. (19), relating to Eqs. (22) and (23), enforces the original limit of the formulae predicting the behavior of undersampled arrays up to the Nyquist frequency. If p is defined as equal to s, then $M_{OPT} = N_{DEG}$ and $N_{OPT} = M_{DEG}$ at the Nyquist frequency, and the assumption does not hold.

Figure 3 shows the calculated maximum, minimum and average MTF for an array with a pitch and sampling aperture of one unit distance. This equates to a fill factor of 100%. It may be seen that the derived formulae agree with sampling theory as the minimum MTF predicted falls to zero at the Nyquist frequency of the above example [Ref. 10, pp. 204–205]. It may also be seen, however, that there could be a considerable device response at this frequency. The variation between the predicted maximum and minimum MTFs is caused by the phase difference between the input signal and the sampling comb. The optimum MTF is yielded when the array is in phase with sinusoidal components of the target, conversely poor performance occurs when the target is out of phase. The figures also show that the variation is predicted to increase with respect to spatial frequency.

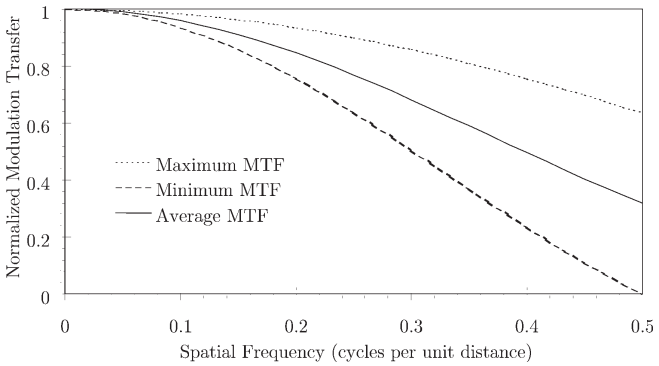

Figure 3. Normalized modulation predicted for an array with a fill factor of 100%. Aperture and pitch are one unit distance.

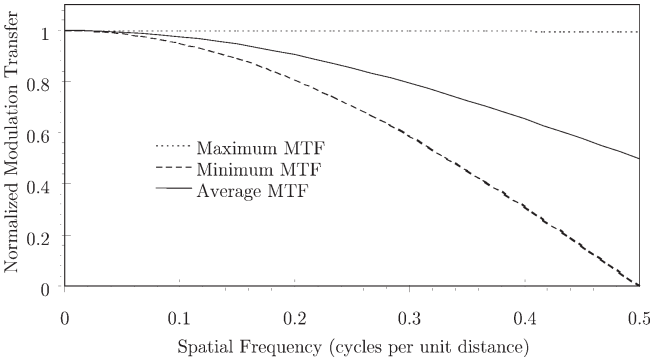

Figure 4. Normalized modulation predicted for an array with a fill factor of 1%. Pitch is equal to 1 and aperture to 0.1 units distance.

The variation may be shown to be exacerbated by the effects of the fill factor. Figure 4 shows the predicted MTF when the aperture of the sampling element is small in comparison to the pixel pitch, i.e., the fill factor is low. It is clearly seen that the formulae predict a large variation in performance, the maximum MTF is much increased. This could be considered an advantage as it increases the value of the average MTF, however the potential for aliasing is also much higher, agreeing with work produced by Kriss.[2]

Intuitively it may be expected that a change in pitch will cause a change in the minimum expected response of a device and indeed this is the case. By plotting results from Eq (23), it may be seen that as the sampling pitch is decreased the predicted minimum geometrical response of the device increases (Fig. 5).

One-Dimensional Line Spread Function

The one-dimensional MTF of a device may be calculated as the modulus of the Fourier transform of the Line Spread Function (LSF).[10] Using the inverse of this relationship it is possible to derive LSFs corresponding to the maximum and minimum MTF using the results above.[10] This is calculated using Eqs. (22) and (23) to describe the MTF, though the variables a and b are

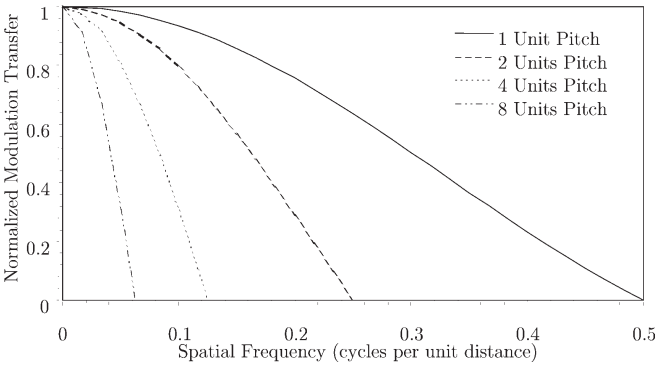

Figure 5. The effect of pitch upon minimum device modulation for an array with a sampling aperture of one unit width.

omitted in order to produce a normalized LSF with an area of unity. Performing this calculation, we found that the maximum and minimum LSF, LSF_{MAX} and LSF_{MIN}, may be represented by:

$$LSF_{MAX} = \frac{1}{s}\prod\left[\frac{x}{s}\right] \tag{26}$$

$$LSF_{MIN} = \frac{1}{2s}\prod\left[\frac{x+\frac{p}{2}}{s}\right] + \frac{1}{2s}\prod\left[\frac{x-\frac{p}{2}}{s}\right] \tag{27}$$

where $\prod[x]$ represents a rectangle function of unit width and height occurring at $x = 0$.

The above result adds confidence to the validity of the formulae. The original derivation method essentially mimmicks the physical sampling process. It may be seen that MTF_{MAX} and LSF_{MAX} agree with the traditional Fourier-based representation usually quoted for a single pixel [Ref. 3, p. 208]. The derivation of MTF_{MIN} and LSF_{MIN} proceeds in the same manner to provide the lower bounds of the performance envelope and should be equally valid if all derivation steps and assumptions hold. The results show that if only the traditional result is quoted, MTF_{MAX}, then discrete device MTF is overestimated. Figures 6(a) and 6(b) represent LSF_{MAX} and LSF_{MIN}. The LSF representative of the average response LSF_{AVE} is given by:

$$LSF_{AVE} = \frac{1}{2}\left(\frac{1}{s}\prod\left[\frac{x}{s}\right] + \frac{1}{2s}\prod\left[\frac{x+\frac{p}{2}}{s}\right] + \frac{1}{2s}\prod\left[\frac{x-\frac{p}{2}}{s}\right]\right) \tag{28}$$

It should be noted that this LSF does not physically occur in the field of view and is merely a conceptual device. A unique feature of the above result is the reduction of the non-stationary nature of a discrete device to a simple combination of rectangle functions representing the sampling behavior of the original pixels. The simplicity of the result warrants the investigation of the non-stationary nature of other pixel geometries.[1]

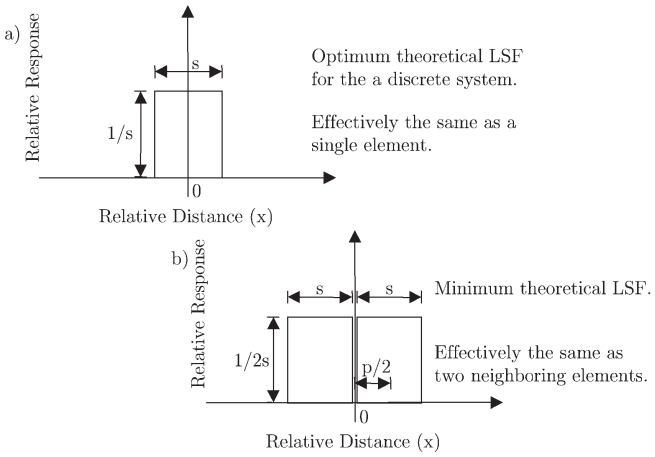

Figure 6. The optimum (a), and the degraded LSF (b), yielded by the work.

Experimental Results and Discussion

In order to confirm the above approach to calculation of non-stationary MTF bounds, a sine wave technique,[11] the ISO Standard 12233[12] and a standard edge gradient technique[13] were used to measure the maximum and minimum MTF as well as the Spatial Frequency Response (SFR) of a Kodak DCS420m monochrome digital camera fitted with a Nikkor 28 mm f/1.8 Autofocus 'D' type lens[14] and a Tiffen infra-red absorbing filter.[15]

The manual accompanying the Kodak DCS420m specifies the sampling pitch of the CCD to be 9 μm.[16] The fill factor, f, and thus the aperture of the CCD is not specified, though a typical value is 90%. Assuming square pixels, this value was used to estimate the aperture width as follows:

$$f = \frac{s^2}{p^2} \tag{29}$$

Therefore,

$$s = \sqrt{f \times p^2} = \sqrt{0.9 \times 9^2} = 8.53\mu m \tag{30}$$

The parameters were used to calculate the expected maximum, minimum and average MTF of the CCD using Eqs. (22), (23) and (25).

The MTF of the lens and filter combination was evaluated using an Ealing Optics EROS 200 system.[17] Radial and tangential measurements were performed on the optical axis of the lens and at angles of 4° 1′55″, 6° 5′53″ and 6° 58′8″ degrees in the field of view. These angles correspond to the edge of the CCD and were used to confirm that optimum performance of the lens coincided with the optical axis.

Additionally, measurements were conducted for the available range of lens apertures. Optimum performance was evaluated by integrating the measured MTF between 0 and 200 cycles per millimeter (c/mm). The maximum was found to occur at f/5.6.

Measurements were performed using tungsten illumination corresponding to that used in the experimental arrangement.

To evaluate the MTF of the camera, test targets were mounted on a 3 m optical bench with an arrangement of

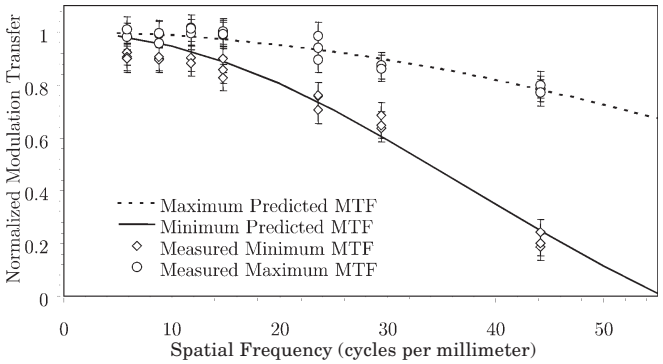

Figure 7. Comparison of predicted modulation and that determined using sine waves for the Kodak DCS420m. Error bars represent ±0.05 modulation.

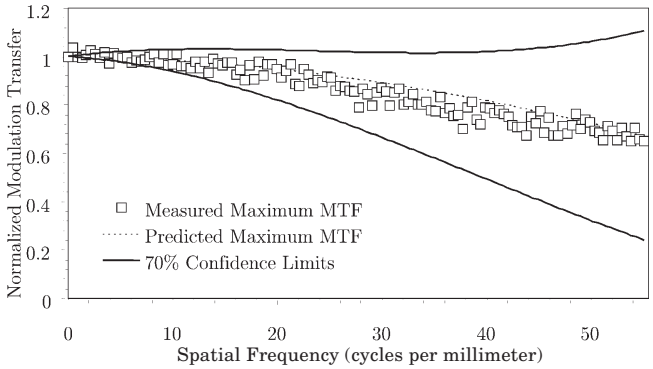

Figure 8. Predicted and measured maximum MTF for the Kodak DCS420m, as determined by the edge technique. See text for explanation of confidence limits.

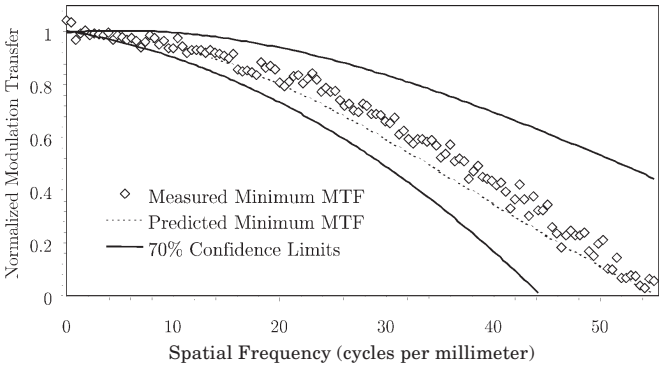

Figure 9. Predicted and measured minimum MTF for the Kodak DCS420m, as determined by the edge technique. See text for explanation of confidence limits.

micro-positioners to adjust translation and rotation in the plane of the target. The stated accuracy of the micrometers was ±2 μm in linear translation and ±5 minutes of arc in rotation. Two Photoflood 200 W tungsten lamps provided even illumination of the target. The DCS420m was rigidly mounted on the optical bench so that the optical axis of the camera was orthogonal to the plane of the target. The distance between the test target and camera was used to calculate the magnification of the arrangement as 1.7×10^{-2}.

After positioning and rotating the target as required, the camera's autofocus system was used to focus. Automated focusing was preferred over manual due to its increased consistency. The lens was set at an aperture of f/5.6 and used in combination with the Tiffen infrared absorbing filter provided with the camera.

The speed setting of the camera was adjusted to ISO 200, the nominal rating of the camera,[16] and the correct exposure determined using the camera meter in spot mode with a Kodak R-27 greycard placed in the plane of the target.

After making exposures as desired, images were downloaded to an IBM compatible PC, via the Adobe Photoshop™ plug-in provided, as 8 bit data. Relevant data was extracted and then converted into effective exposure units[6] using the tone reproduction characteristics of the device determined using a Kodak Q-13 greyscale under the same conditions. The MTF of the system was calculated using the recorded images according to the details given later for each method. The component of the lens MTF was removed from the determined MTF in the usual manner.[10]

Figure 7 shows the results of MTF determination using sine waves compared with the model prediction. For each imaged sine wave, the first differential of the recorded patch was calculated. Maxima and minima in each line of the image were detected by locating zero crossing points of the first derivative. The modulation was then calculated using the extreme values of the detected points after conversion into effective exposure units. Correction for the modulation of the original sinusoidal target and that of the lens at the spatial frequency in plane of the detector was then applied to yield the modulation transfer at each spatial frequency.

Error bars are shown representing ±0.05 modulation. This is an estimated measurement error derived from the lens MTF determination and nominal modulation of the sinusoidal test target. Error in the determined lens MTF at a given spatial frequency is estimated as ±0.03 modulation.[17] This has to be rescaled, however, as the nominal modulation of the sinusoidal target is 0.6 and both values are used in combination to correct the derived MTF. This yields a minimum error in determination of the modulation striking the CCD of 0.03/0.6 = ±0.05. As the modulation measured from the CCD falls, error in the result will proportionally rise beyond this and errors should be considered as underestimated in this case.

Figures 8 through 11 show MTF as determined using ISO 12233 and a standard edge technique. The edge target used was produced using a Hewlett Packard 6MP laser printer. To avoid effects caused by halftoning, the edge was arranged in the direction of printing and designed to have a transition from the maximum possible density to page white. A number of measurements were made along the length of the edge to ensure a consistent density. The use of a laser printed edge, while not ideal, is possible because of the low magnification of the system that ensures the frequency response of the target is constant over the desired range. This may be confirmed easily using reflection microdensitometry.

The target was positioned in the center of the field of view of the camera. Exposures were made and examined in order to align the orientation of the target with the CCD array. Images were made, using the procedure described above, translating the target in 50 μm intervals with the micro-positioners. This corresponded to

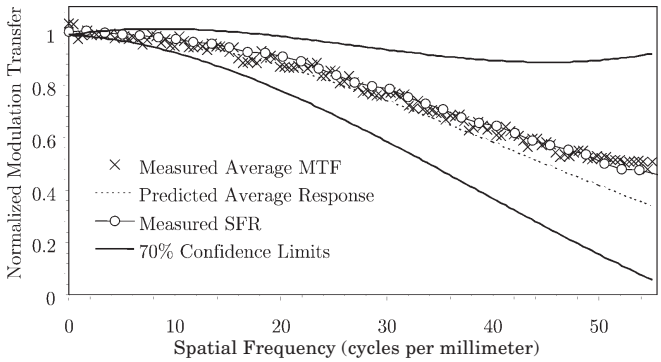

Figure 10. Predicted and measured average MTF with SFR results for the Kodak DCS420m. Determined using ISO 12233 and the edge technique. See text for explanation of confidence limits.

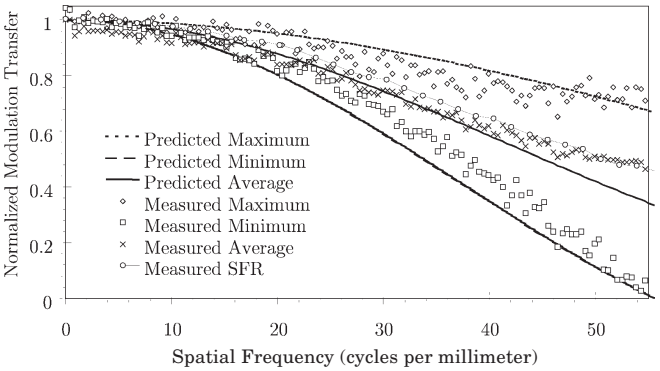

Figure 11. Predicted MTFs compared to those measured using the edge gradient and ISO 12233 standard measurement techniques.

the image of the edge advancing 0.85 μm across the CCD. The images were then downloaded and corrected as above. A mean edge profile was extracted from each by averaging image columns in order to reduce noise. MTFs were calculated in the usual manner[7] and the maximum and minimum response selected. This was achieved by evaluating the integral of the determined MTFs between the DC component and the Nyquist frequency of the device.

In addition all responses were averaged to produce a mean. To calculate the SFR of the device, the above target was rotated approximately 5° and an exposure made. This image and the previously calculated transfer function were used as the input image and Opto-Electronic Conversion Function (OECF) for the ISO 12233 software.[18] All results were corrected for the component of lens MTF and compared to those predicted.

The figures show curves representing 70% confidence limits as calculated by Yeadon, Jones and Kelly.[19] Yeadon and coworkers have shown that noise adds a linearly increasing component to the measured MTF and that whilst this component cannot be used to correct measured curves, it may be used to estimate errors in the results.[19]

The Fourier transform of the LSF is calculated as usual. The technique first requires that any linearly increasing component in the Phase Transfer Function (PTF), caused by an incorrect choice of origin, be removed. This is achieved by integrating the PTF between

Table I. Correlation between Experimental Measured Values of MTF for the Kodak DCS420m and thos Predicted Using the Mathematical Model.

Curve	Correlation Coefficient (r^2)
Maximum MTF	0.8306
Minimum MTF	0.9646
Average MTF	0.8978

the DC component and an arbitrary frequency, ω_K. The value of this integral indicates that a linearly increasing or decreasing function needs to be added to the PTF to reduce the integral to zero. Using the corrected phase, $p'(\omega)$, modified real and imaginary components, $r'(\omega)$ and $i'(\omega)$, are calculated:

$$r'(\omega) = m(\omega)\cos\left[p'(\omega)\right] \tag{31}$$

$$i'(\omega) = m(\omega)\sin\left[p'(\omega)\right] \tag{32}$$

where $m(\omega)$ is the modulus of the original Fourier transform at spatial frequency ω. Considering symmetry, the real and even LSF will produce a real and even Fourier transform in idealized conditions [Ref. p. 102]. Yeadon and co-workers show that any imaginary component of the transform is therefore statistically related to the noise in the transform.[19] The semi-angle, $\alpha(\omega)$, of the imaginary component is calculated at each spatial frequency:

$$\alpha(\omega) = \frac{\tan-1\left[i(\omega)\right]}{\omega} \tag{33}$$

The root-mean-squared value of the semi-angle, α_{RMS}, is then calculated:

$$\alpha_{RMS} = \left[\frac{1}{\omega_K}\int_0^{\omega_K} \alpha(\omega)^2 d\omega\right]^{\frac{1}{2}} \tag{34}$$

where all variables take their previous definitions. Yeadon and co-workers recommend that the above procedure is repeated for varying values of ω_K, the maximum frequency considered.[19] Overestimation of the confidence limits is avoided by employing the lowest value of α_{RMS} calculated for values of ω_K between 1/4 and 3/4 of the estimated cutoff frequency of the system being measured. The MTF of the system is then defined by Yeadon and co-workers[19] as:

$$MTF(\omega) = r'(\omega) \pm c(\omega) \tag{35}$$

where $c(\omega) = \omega \tan [\alpha_{RMS}]$. Yeadon and co-workers state that the calculated limits provide a 70% probability of including the real value at each point.[19] Limits for Fig. 10, the average MTF, are calculated using a single curve.

Figures 7 through 10 show some degree of correlation between the predicted and the determined values, Table I. Initially, the result confirms the non-stationary nature of discrete devices merely by the existence of a difference between maximum and minimum responses. All figures confirm that this difference is seen to increase with spatial frequency as the model predicts. Results calculated using sinusoidal and edge techniques show some agreement.

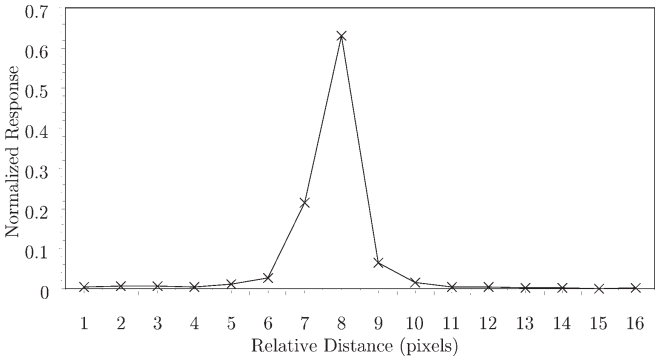

Figure 12. A magnified portion of a trace of the LSF of the Kodak DCS420m in combination with the Nikkor 28 mm lens.

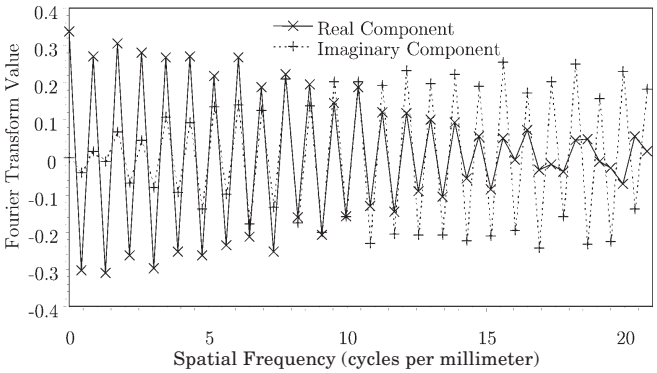

Figure 13. A magnified portion of the Fourier transform of an LSF trace of the Kodak DSC420m and Nikkor 28 mm lens, showing oscillation of real and imaginary components.

Experimental errors will exist for a multitude of reasons. Translation of the test targets may not have been of sufficient subtlety to invoke the actual maximum and minimum response of the array. Other test target positioning errors may also exist due to angular rotation of the targets and errors present in the micropositioners used.[20] Variation in the MTFs produced due to rotation of test targets is examined briefly in Refs. 21 and 22. Intra-pixel sensitivity variation has been shown to exist.[23] Generally light sensitivity drops towards the edges of individual elements. The effect is not accounted for in this model and will contribute to the MTF of the device.

No account has been made for the effect of an optical pre-filter or system electronics. As these effects increase for a given system, the MTF will depart from the geometrical component. Furthermore, inaccuracies may be contained in the predicted MTFs due to the use of an estimated value of aperture and determination of the lens MTF as previously mentioned.

The mean measured edge MTF of the Kodak DCS420m corresponds well with the determined SFR of the device as well as the predicted average response. This supports suggestions that conceptually SFR measurement may be thought of as an average system response.[24] The slight bias in the determined curves as spatial frequency increases may be accounted for by the effects of noise as detailed by Blackman[25] and Yeadon and co-workers[19] or those of aliasing [Ref. 10, p. 107].

The 70% confidence limits of Yeadon and co-workers overlap significantly for the maximum and minimum MTFs calculated, Figs. 8 and 9. Using this the model would not be confirmed definitively as a true description of discrete system behavior. This dismissal of the results, however, must be tempered by consideration of the calculation methodology for the limits.

The technique for calculation of the limits was engineered in 1970 with analog edge measurement under scrutiny. Microdensitometer scans of analog edges provide the opportunity for vastly oversampled traces. This reduces the effects of the discrete nature of the traces, such as aliasing, and provides an opportunity to ensure that the LSF of the measured device is sampled using a large number of data points. These opportunities are not provided for when determining the LSF of a CCD and all traces are undersampled. Figure 12 shows that the LSF of the Kodak DCS420m and lens with any significant information content may only occupy between 7 and 10 pixels.

The low number of points makes choosing an appropriate origin for the Fourier transform difficult at best. Even with the utmost care, the origin of the LSF of the lens-CCD combination will fall either side of a sampled point in the majority of cases. This slight shift of the origin introduces oscillation of the real and imaginary components of the Fourier transform, Fig. 13. This in turn causes the calculated value of α_{RMS} to be increased.[19]

Zero-padding the LSF traces does not reduce this effect as no new information is added to the signal. Interpolation of the LSF to provide intermediate sampled points and an estimation of the origin of the LSF is also not feasible. This is because the noise that provides information for the error estimation will be modified significantly by the interpolation function. The only reasonable strategy is to accept that the 70% confidence limits will be over estimated and consider this when evaluating results. If the general agreement of the measured, predicted and sinusoidal curves is considered the approach appears reasonable.

Conclusions

Work has been presented which shows that a description of the non-stationary behaviour of discrete devices may be reduced to simple analytical expressions describing the maximum and minimum MTF of the device. Further, it has been shown that these expressions are simple combinations of the original response characteristics of an individual pixel.

Significantly, it is shown that the traditional sinc based description of device MTF is the maximum that may occur and possible device response is thus always overestimated. Therefore, the minimum device response, described here, is a better parameter to include in the design of critical systems.

The derived formulae have been experimentally tested against a CCD device using sine wave, edge and the ISO 12233 measurement techniques. The formulae show agreement with the results.

References

1. T. Hase, Two dimensional modulation transfer function of luminance on display images with a mosaic pixel structure, *IEEE Transactions on Consumer Electronics* **40**(2), 83–91 (1994).
2. S. Honjo and M. Kriss, Image structure and evaluation, in *Handbook of Photographic Science and Engineering*, C. N. Proudfoot, Ed., IS&T, Springfield, VA, 1997, Chap. 17.
3. G. C. Holst, *CCD Arrays, Cameras and Displays*, SPIE Optical Engineering Press, Bellingham, WA, 1996.

4. S. Mehra, P. Hung, H. Haneishi, and Y. Miyake, On the evaluation of different imaging systems: Two-dimensional MTF for digital scanning systems, *Proc. 9th International Congress on Advances in Non-Impact Printing Technologies*, IS&T, Springfield, VA, 1993, pp. 479–482.
5. D. N. Sitter, J. S Goddard, and R. K. Ferrell, Method for the measurement of the modulation transfer function of sampled imaging systems from bar-target patterns, *Appl. Opt.* **34**(4), 746–751 (1995).
6. J. L. Smith, Modulation transfer function for a CCD array with sample-and-hold operation on static waveforms, *SMPTE Journal*, 465–467 (1995).
7. H. Wong, Effect of knife-edge skew on modulation transfer function measurements of charge α-coupled device imagers employing a scanning knife edge, *Opt. Eng.* **30**(9), 1394–1398 (1991).
8. J. C. Feltz and M. A. Karim, Modulation transfer function of charge-coupled devices, *Appl. Opt.* **29**, 717–722 (1990).
9. N. Balram and W. P. Olson, Lower Bound for CCD Image Quality, *Proc. SPIE* **2651**, 108-116 (1996).
10. J. C. Dainty and R. Shaw, *Image Science; Principles, Analysis and Evaluation of Photographic Type Processes*, Academic Press, London, England, 1974.
11. R. L. Lamberts, Use of Sinusoidal Test Pattern Arrays for MTF Evaluation, *Engineering Notes, Sine Patterns*, New York, New York, USA.
12. ISO/FDIS12233:1999(E), *Photography-Electronic Still Picture Cameras-Resolution Measurements*, International Organization for Standardization, New York, New York, USA, 1999.
13. E. C. Yeodon, *Edge Gradient* Analysis, The Perkin-Elmer Corporation, Norwalk, Connecticut, USA, 1969.
14. Nikon UK Ltd., *Nikon 28 mm Lens Guide*, Nikon House, Kingston-upon-Thames, Surrey, UK.
15. The Tiffen Company LLC., Hauppauage, New York, USA, 1996.
16. Eastman Kodak Inc., *Kodak DSC420m Camera Users Guide*, Rochester, New York, USA, 1996.
17. Ealing Electro-Optics Plc., EROS 200 Users Guide, Watford, Herts, UK, 1980.
18. *MATLAB Computation, Visualisation, Programming*, Version 5.3, MathWorks, Inc., Natick, MA, USA, 1997.
19. E. C. Yeadon, R. A. Jones and J. T. Kelly, Confidence Limits for Individual Modulation Transfer Function Measurements Based Upon the Phase Transfer Function, *Photogr. Sci. Eng.* **14**(2), 153-156 (1970).
20. Ealing Electro-Optics Plc., Ealing electro-optics catalogue, Watford, Herts, UK, 1997.
21. R. B. Fagard-Jenkin, R. E. Jacobson and N. R. Axford, A Novel Approach to the Derivation of Expressions for Geometric MTF in Sampled Systems, *Proc. of IS&T's 1999 PICS Conf.*, IS&T, Springfield, VA, USA, 1999, 225-230.
22. R. B. Jenkin, On the Application of the Modulation Transfer Function to Discrete Imaging Systems, PhD Thesis, University of Westminster, Harrow Campus, Harrow, UK, 2002.
23. M. Okigawa, A New and Simple Test Structure for Evaluating the Sectional Photosensitivity of Pixels in a Frame-Transfer CCD Image Sensor, in *Proc. IEEE 1992 International Conf. on Microelectronic Test Structures*, IEEE Press, Los Alamitos, CA, USA, 1992, pp. 134-138.
24. R. B. Fagard-Jenkin, R. E. Jacobson and N. R. Axford, A Novel Approach to the Derivation of Expressions for Geometrical MTF in Sampled Systems, *Proc. IS&T's 1999 PICS Conf.*, IS&T, Springfield, VA, USA, 1999, pp. 225-230.
25. E. S. Blackman, Effects of noise on the Determination of Photographic System Modulation Transfer Functions, *Photogr. Sci. Eng.* **12**(5), 244-250 (1968).